

Interpretation of nonlinearity in wind generated ocean surface waves

M J Varkey

Physical Oceanography Division, National Institute of Oceanography, Dona Paula, Goa 403 004, India

Received 12 December 1991; revised 22 February 1993

This study attempts to resolve a mix-up between a physical process and its mathematical interpretation in the context of wind waves on ocean surface. Wind generated wave systems, are conventionally interpreted as a result of interaction of a number of sinusoidal component waves; a consequent idea arising out of Fourier analysis. It is hypothesised that a sea state which is always nonlinear to various degrees is a result of interaction, both linear and nonlinear, between nonlinear component waves of different nonlinear intensities and their groups. The intensity (nearly linear to high) and dominance of a particular component wave depend on the stage of development of sea state, wind structure and environmental conditions like currents, bottom topography and other wave systems. As the nonlinearity of a sea state becomes more and more, the sinusoidal (linear) component wave model becomes more and more unfit and the nonlinear component wave model becomes more appropriate. Earlier works with results as pointers to the hypothesis are critically examined. Four largely different deep water sea states are analysed for their bispectra and bicoherence and the results are found to support strongly the nonlinear component wave model.

While studying the basic aspects of growth of sea states, i.e. energy induction by wind onto the sea surface, growth of height and period and nonlinear energy transfer between linear component waves (CWs), the vital physical aspect to be kept in view is that the sea state is always nonlinear to various intensities and the assumption of stationarity is a simplification for obtaining results for immediate applications. For understanding the basic physical processes one should start at the initial stage of transfer of energy from wind by instantaneous impulses (short period) and sustained pulses (long period) and not by assuming simple, perfectly sinusoidal, dispersive CWs, but by providing options for all types (linear and nonlinear) of wavelets (or primary waves) and their groups (Fig. 1a); no wind impulse can stop itself by producing a single wavelet alone, it is always wavelets and their groups. It is theoretically and intuitively correct that these wavelets and groups are always nonlinear to various degrees, but, they can generally be approximated to linear CWs. Intensity of nonlinearity in these wavelets and their groups depends on wind structure and nature of the energy imparting mechanisms. The physical characteristics of these primary waves undergo large changes as the sea state grows more by the wind-wave coupled energy transfer mechanism. Now, it is easy to visualise the generation and growth in a holistic, total perspective. The innumerable sur-

face forcings of different types (coupled and uncoupled) from wind generate innumerable number of wavelets and their groups of various nonlinear types and intensities which interact among themselves, linearly and nonlinearly, and with wind to cause a chaotic sea state as the wind grows.

The complete regime of wind waves on different environments from initial wavelets to breaking waves can be analytically modelled by 4 wave theories (see Figs 2-7 in *Shore protection manual* also). They are: (1) linear Airy waves, (2) nonlinear Stokes waves, (3) nonlinear cnoidal waves,

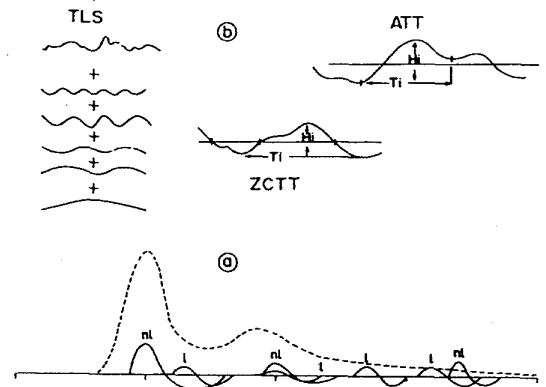


Fig. 1-(a) Schematic spectrum with different types of component waves (n.l.=nonlinear and l=approaching linear).
(b) Different methods of computing spectra

and (4) nonlinear solitons, of which the 1st and 4th are limiting cases of cnoidal waves. These analytical models do not represent either a full sea state or a single wave as observed at the sea surface, but can be considered to represent approximately significant or dominant waves in the spectral peak domain of the variance spectrum. From the above referred figures in *Shore protection manual*¹, it can be seen that the region around a hypothetical line from 0.4 (d/gT^2) (d =water depth, g =gravity acceleration) to 0.0005 (H/gT^2) (H =wave height, T =wave period) is able to represent the dominant waves from initial generation to breaking by shoaling in shallow waters. Similarly, the region around a second hypothetical line from 0.4 (d/gT^2) to 0.05 (d/gT^2) along the upper boundary, is able to represent the dominant waves from initial generation to breaking in deep water. This explanation arises out of the original hypothesis that the CWs in a sea state are not purely sinusoidal but are always nonlinear, which can sometimes be approximated to linear sinusoidal waves. Hence, in shallow water CWs would be Airy waves, cnoidal waves and solitons whereas in deep water they would be Airy waves, Stokes' waves and solitons when subjected to nonlinear Fourier analysis² in which the

recorded sea state is decomposed into different nonlinear CWs with nonlinearities varying from 0 (sinusoids) to very high values (solitons).

As a consequence of the above theoretical concept the following modes of interactions are possible on sea surface between different types of CWs:

Component wave	Interaction mode	Intensity of nonlinear transfer
Linear	Linear	Zero
Linear	Nonlinear	First degree
Nonlinear	Linear	First degree
Nonlinear	Nonlinear	Second degree

The currently available energy transfer models for wind waves (Fig. 2) incorporate only the first 2 processes as shown in the above scheme. The third and fourth are yet to be studied. While the third would produce an additional first degree energy transfer the fourth produces a second degree transfer. This increased (by an order of magnitude) nonlinear activity may explain many features³⁻¹⁵ related to spectral shape, its growth and nonlinear transfer, differences observed in laboratory and field experiments, dispersion relationships, overshoot, etc.

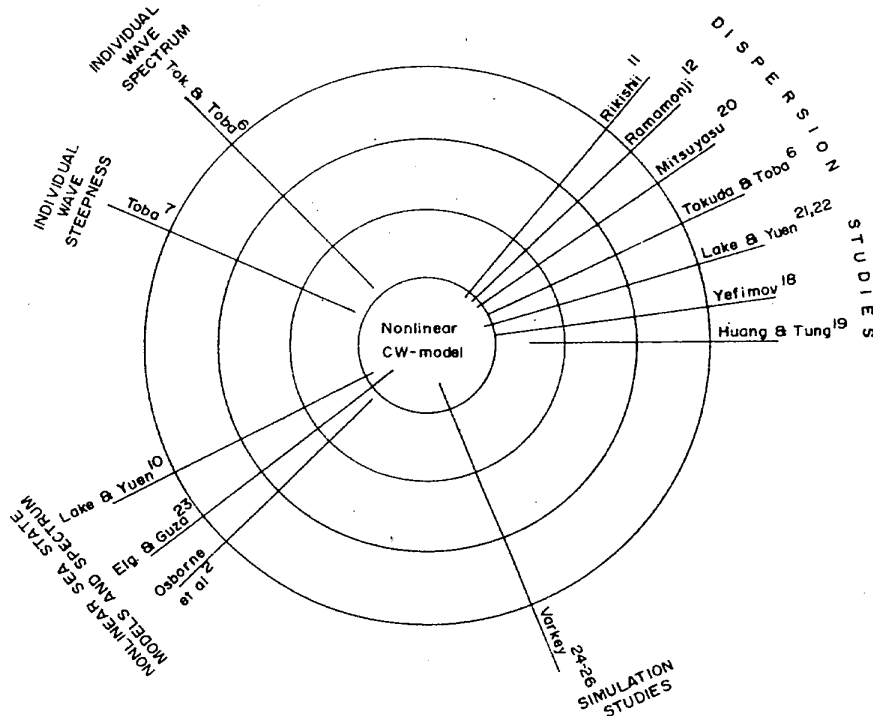


Fig. 2 - Surety chart showing the different studies pointing to the nonlinear CW model

Earlier studies—Toba⁷ after reviewing works related to initial generation of wavelets, wind stress, turbulence and convection, dispersion relationship, etc. proposed that the main phase of growth of wind waves is a strongly nonlinear process. He observed that the steepnesses of the apparent individual waves (from trough to trough) is approximately constant and explained this as due to strong nonlinearity of the sea state (see Lake & Yuen¹⁰ also). It is easy to explain Toba's concept of strong nonlinearity to result from the present proposition that the CWs themselves are nonlinear. When the CWs at the spectral peak regime are nonlinear and constitute the dominant waves, the steepnesses of individual waves (IW) would be approximately constant.

Tokuda & Toba⁶ showed that the traditional linear spectra (TLS) and the 2 trough to trough spectra (TTS) are very different for the same laboratory wave records (see Fig. 1). The difference is in the presence of a secondary peak at 2^*f_p in TLS where f_p is the spectral peak frequency. This peak is absent in TTS. This observation can be explained as a result of the CW or CWs at or around f_p being strongly nonlinear. This nonlinear (say similar to a Stokes wave) component in the TLS would be represented by a second harmonic spectral peak at 2^*f_p as observed by Tokuda & Toba⁶. In the case of ZCTT, one subset of TTS (Fig. 1), while measuring the parameters of the IWs, identified by zero-crossings, only the major or dominant waves are taken into consideration. In the case of ATT (second subset of TTS) smaller waves riding over bigger ones are also considered (see Fig. 1b). In both cases, the measuring technique assigns a varying mean water level from wave to wave compared to the mean water level taken over the full sea state as for TLS. This effectively incorporates into the IWs, features like crest and trough asymmetry in both horizontal and vertical, arising out of nonlinear processes, transforming them into nonlinear CWs. This technique suppresses the second harmonic peak at 2^*f_p in both types of TTS. It is to be clearly noted that the frequency axis of the TTS represent frequencies of nonlinear CWs, quite different from that of TLS. Toba⁷ pointed out that the TLS and TTS (from ZCTT) represent better the low frequency side of the triangular spectral peak regime while the TTS from ATT represent the high frequency side better. This feature can also be explained as resulting out of the shifting mean water level in the two methods which samples the low frequency and high frequency CWs differently.

Anomalous features were observed experimentally in phase speeds of wind waves in comparison to those of Fourier decomposed linear CWs by many workers^{6,7,10-13,15-19}. Tokuda & Toba⁶ showed that the phase speeds of Fourier decomposed CWs estimated using cross-spectral analysis and those of IWs delineated using zero-crossing trough to trough (ZCTT) method agreed well around the spectral peak. The estimates for higher frequencies ($>f_p$) showed differences. Also, estimates for both the regimes ($\sim f_p$ and $>f_p$) were much larger than the values given by the linear theory. The deviations from linear theory were consistent for all frequencies, increasing towards higher frequencies, and were explained as due to the effect of wind drift^{7,11,12,20}. The phase speeds of CWs around 2^*f_p were the same as that at f_p . This is explained as due to presence of considerable second harmonic contribution of the dominant nonlinear CWs (Stokes type) at f_p . The absence of a secondary peak at 2^*f_p for phase speeds estimated from IWs arises out of the nonlinear nature of the IWs themselves treated wholly and not in decomposed components. Tokuda & Toba⁶ showed that the phase speed distributions of CWs differ with fetch for higher frequencies ($>f_p$). The wavy nature of the curve for a fetch of 5.87 m (the largest) seems now to be due to the increased effect of nonlinear CWs at f_p and at higher frequencies coexisting with free CWs with varying intensities. The uniform nature of the curve for a fetch of 1 m (the shortest) seems to be due to the less developed nature of the nonlinear CWs at f_p and at higher frequencies. The dominance of nonlinear CWs at f_p and other frequencies grows with the stage of development of sea state. Also, the increase in phase speeds over the same frequency regimes ($>f_p$) with fetch can be explained now as due to increase in nonlinearity of CWs (in laboratory) bringing in more amplitude dispersion and wave drift.

Masuda *et al.*¹⁶ provided a theoretical framework for examining the dispersion relation in comparison to nonlinear CWs. Their experimental results on measured phase velocity and coherence showed clearly that their nonlinear model of 2 dimensional waves is the best fit to the observed values for waves outside the generating area free from wind drift²⁰. A nonlinear one dimensional model by Tick (see ref. 20) also predicted the phase velocity well but failed to explain the coherence pattern. This seems to be a normal consequence of the short crested, 2 dimensional wave system in which the coherence can become vague due to change in the structure of coexistence of

bound and free CWs. This is apparent in the results of Tokuda & Toba⁶ also. Mitsuyasu *et al.*²⁰, like some other workers found that their linear 2 dimensional theory of random waves gave fairly good agreement with measurements for the dominant energy containing part of the spectrum near f_p . They explained the observed rapid increase of phase velocity and the corresponding local decrease of coherence at about 1.8 (f/f_p) to coexistence of free and bound CWs. They also suggested that many dominant nonlinear CWs can exist in the frequency range of $0.9 < f/f_p < 1.5$.

Ramamonjjarisova *et al.*¹² computed wave celerities corrected for wind drift and mass transport using the method of cross correlation. They found that the lowest celerity in the low frequency range ($< f_p$) is close to half the celerity at f_p and explained this as a result of wave groups in the sea state. After considering their results in relation to nonlinear CWs they finally noted that a sea state during its propagation and interaction with the wind field could be more appropriately regarded as a random field of nonlinear CWs and their groups rather than a superposition of free CWs. Rikiishi¹¹ also obtained very similar results from laboratory studies on phase velocities and considered them of great importance in understanding the substance of spectral CWs in the laboratory. Now, in this study these results are thought to lead to the present hypothesis. Huang & Tung¹⁹ found that a single form of dispersion relation is not suitable for all wave conditions. They also noted that in the case of a single train of waves, as a simplified case of their nonlinear random gravity sea state, the phase velocity is the same as that of a Stokes nonlinear type wave. Yefimov¹⁸ also, like previous workers, concluded that the high frequency range of the spectrum consists of both bound and free components. His results indicated that the bound components are not negligible.

Lake & Yuen¹⁰, after theoretical and experimental investigations^{21,22} on evolution of nonlinear wave trains and on some of the above discussed nonlinear characteristics of sea states like dispersion relation, steepness properties, modulation instability, etc. with coalescent results, proposed a nonlinear 'dominant wave model'. In this model, for steady wind blowing in one direction, a nonlinear wind wave system was completely characterised by a single nonlinear wave train having a primary frequency equal to f_p and other high frequency and less significant free waves. A few important and relevant results are as follows: (1) the dominant wave alone received almost all

of the wind energy (see discussion in a later section also), (2) the evolution of a real sea state spectrum is considered to be achieved by the sustained wind input to the dominant nonlinear wave and by its modulation instability changing the carrier frequency, (3) even though nonlinear sea waves may have properties similar to Stokes type waves, they cannot be well modelled, individually or in groups, using properties of Stokes waves, since they are highly modulated and unsteady (this supports the hypothesis that the nonlinear CWs are of different nonlinearities), (4) the effect of nonlinear CWs is predominant over the effect of randomness of phases. This result seems to acquire special significance in the proposed modes of interaction (see introduction) in the case of nonlinear or coupled interaction of nonlinear CWs resulting in a second order transfer which would help the growth of modulation instability.

Osborne *et al.*² computed a nonlinear spectrum of laboratory generated random waves by inverse spectral transform. Based on the results they proposed that a nonlinear wave field or wave train may be described as a linear superimposition of nonlinearly interacting sine waves, Stokes waves, cnoidal waves and solitons. It is noteworthy that this proposition also allows a second order nonlinear transfer by nonlinear interaction of nonlinear CWs as described in the introduction. When Osborne *et al.*² proposition is compared with the third result of Lake & Yuen¹⁰, it becomes evident that the nonlinear CWs themselves are of different natures, but at present are modelled by Stokes or cnoidal waves only. The present hypothesis is supported directly by this finding.

Elgar & Guza²³ found that a nonlinear model based on the Boussinesq equations for waves on a shallow, sloping bottom accurately predicts the observed bispectral evolution (involving bicoherence, biphasic and surface elevation skewness and asymmetry) compared to results from a linear finite depth model. Eventhough, they applied the nonlinear model specifically to shallow water waves only, wherein nonlinearities are thought to be large, the results in association with other studies discussed in previous paragraphs, suggest that nonlinear CW models would be better generalised solutions for all situations. The results from deep water waves presented in Results and Discussion part prove the same.

Varkey²⁴ by a numerical simulation showed that the kurtosis values computed from simulated surface wave profiles with phase coherency (equal phases) at f_p are considerably high suggesting increase in nonlinearity with phase coherency. In-

crease in kurtosis values were also noted²⁵ when the phase values were equal to f_p and $2*f_p$ over half energy band widths. These results brought out the possibility of highly nonlinear sea states and nonlinear component waves to arise due to phase coherency between component waves. It was also shown by another simulation²⁶ of bispectra that the component waves in a sea state are linear and nonlinear and over the spectral peak regime they are highly nonlinear.

Bispectrum and nonlinearity—Hasselmann *et al.*²⁷ in a pioneering work, found good agreement between observed results and theoretically derived values in the case of interaction between spectral peak and other frequencies. Houmb²⁸ computed bispectra of recorded waves and Stokes nonlinear waves and concluded that the bispectrum and skewness are good measures of deviations of the sea surface from Gaussian distribution. Kim & Powers²⁹ showed the bispectrum to be a very useful diagnostic tool for studying nonlinear interactions in random processes. They also showed that a normalised bispectrum, the bicoherence spectrum, can be used to discriminate between nonlinearly coupled waves and free waves by delineating simulated quadratic coupling in an artificial time series data. Elgar & Guza³⁰ used the bicoherence spectrum to study the nonlinear evolution of sea surface waves on a shoaling coast. The application of bicoherence method to a continuous spectrum as observed in the case of sea waves would conclusively resolve only second order interaction modes between spectral peak and other peaks or harmonics. In a continuous spectrum higher order interactions are always present but would be largely unresolvable in the bicoherence analysis. In view of the above empirical results, a set of deep water wave data were analysed for bispectrum and bicoherence in support of the proposed hypothesis and the details are presented elsewhere.

Materials and Methods

Wave data were recorded using a ship-borne wave recorder on board *R.V. Gaveshani*. The sensors were fixed at a depth of 2.1 m below mean water level and are reliable only within the frequency range 0.05 to 0.33 Hz. Data were recorded for 15 min duration at 2 places where water depths were 250 and 500 m, off the east coast of India at about 16°30'N from 24 September to 4 October 1980. These records were digitised at 1 sec interval and the resulting data series were used. Even though wave records data series were available for about 900 sec, digitised values were always

around 800 points due to recording problems. Hence, a total record length of 768 sec, resulting in 6 sub-profiles of 128 digitised values, was used for the computation of bispectrum (see Fig. 3) and bicoherence. Considering a maximum spectral period of 16 sec, observed from the present set of data (see Figs 4-7), a profile length of 128 sec would have 8 full waves of the spectral peak period. This is found to be quite good for bispectral computations, especially in view of Borgman's³¹ results. He found that some large spectral density values associated with the spectral peak disappeared in the next spectrum computed from a second data series after 20 min, each computing segment being of 13.6 min duration, showing the intensity of energy transfer processes within the wave field. Hence, long records can mask the finer details very much. The autospectrum, bispectrum and bicoherence were estimated following the methods used by Kim & Powers²⁹ except for the following differences. A cosine tapering at both ends of the sub-profiles was applied to reduce leakage³². Bispectra (modulus values) thus computed for each sub-profile were smoothed by arithmetic averaging on a grid (3×3) all over the bispectral quadrant. The final bispectra were obtained by taking the average of the 6 independent smoothed estimates (profile averaging) from the 6 sub-profiles resulting in number of degrees of freedom (DF) of 108. A similar procedure was used by Elgar & Guza³⁰ also to increase the stability of the bispectrum. The final smoothed autospectra were computed by averaging the independent estimates from the 6 sub-profiles resulting in only 12 DF. This accuracy is low compared to that of the bispectrum. But a close look at the autospectrum of wind waves shows that smoothing by running averaging to increase the DF, filters out many of the fine features of the spectrum which can suggest clues to higher order interactions. Hatori⁵ showed that autospectrum averaged over many sub-profiles retains much of the finer structures compared to one smoothed by running averaging. A comparison of the autospectrum shown in Fig. 5 with another computed using a longer (X4) profile of N=512 data and smoothing by running averaging of 11 points (DF=22) showed that the present method of smoothing for autospectrum with high resolution is better for interpretation of bispectrum and bicoherence. As the present method is limited to quadratic coupling only, profile smoothing alone is considered to be optimum. This is shown to be correct in Fig. 4c in comparison to the peak of the spectrum of a sine curve.

All autospectra are corrected for an average noise level computed as the mean of the raw spectral densities from 0.4 to 0.5 Hz.

A calibration check of the computing procedure by a sinusoidal profile showed that the autospectral peaks have optimum resolution at present (Fig. 4c). A blank noise level of 0.2 for the bicoherence spectrum was determined using a sinusoidal profile as input data and is found to agree with the values of the 25th peaks of the different bicoherence spectra computed from all wave data sets. A comparison of the present computing procedure with that of Kim & Powers²⁹ with an identical test profile showed a bicoherence maximum of 0.9 instead of 0.99 (maximum is 1) of Kim & Powers²⁹. This minor difference is due to the dependency of the bicoherence peak on the leakage reduction filter and the Gaussian noise added (both were different in the present study). It is worth noting that a 50% reduction in the Gaussian noise level increased the value of the bicoherence peak to 0.96, but changed the minor peaks of the bicoherence spectrum.

Four sample sea states namely B01, B07, B10 and B17 (see ref. 25 for real profiles) have been selected for this study for the following reasons. B01 represents a dominant swell with very minor high frequency components (Fig. 4); the peculiarity being that the spectral peak is constituted by a single component wave. B10 is a wide band, multi-peaked (3 peaks) swell dominated sea state with 3 dominant component waves (Fig. 5). B17 is multi-peaked (3 peaks), but the peaks are wider compared to B10 and are constituted by more than 1 component wave (Fig. 6) with much less swell energy. B07 is a double peaked sea state with dominating local sea (Fig. 7).

Results and Discussion

Table 1 presents all important bispectral, bicoherence and autospectral peaks and approximate noise levels of all wave profiles. It is important to note that many of the peaks in the bispectra have considerable cross sections at the peaks permitting interaction of some other combinations of CWs other than those entered in the table whose amplitudes are much less than the entered autospectral peaks. The bispectrum would resolve quantitatively only the quadratic interactions of the first order. But second order interactions would also be qualitatively represented as discussed later. As sea states are always nonlinear, weakly or strongly, nonlinear interaction is possible between different CWs (linear or nonlinear) and the intensity of interaction depends on ampli-

tudes of CWs, and relations of phases and frequencies; harmonic couplings giving maximum nonlinear effects. Nonlinearities can be due to presence of a single dominant nonlinear CW as proposed by Lake & Yuén¹⁰ and demonstrated on a Stokes' nonlinear profile by Houmb²⁸. Hence, a bispectrum alone would fail to resolve between peaks due to a nonlinear CW and due to nonlinear interaction of linear CWs. This problem can be solved partly by bicoherence spectrum which measures intensity of bound (nonlinear) CW power to free (linear) CW power. By studying the peaks of bispectrum, bicoherence and autospectrum, it is possible to identify the dominant linear and nonlinear CWs. A comparative study of Table 1 and the figures (Figs 3-8) is carried out in the following section for the different profiles.

Profile B01—All the bispectral peaks (Fig. 3) except the one at (0.25, 0.066) have sufficiently wide peak cross sections at the highest or one contour below to include either the higher harmonics (0.14 and 0.206 of the main CW peak at 0.065 Hz or low amplitude nonlinear CWs at 0.078, 0.094, 0.159, 0.228 and 0.275 Hz. The largest bispectral peak at (0.092, 0.066) includes a peak to peak interaction centered around (0.065, 0.065) and interactions of minor nonlinear CW or CWs centered at 0.094 and 0.078. Since the bispectral maximum is centered at (0.092, 0.066), the low amplitude CW or CWs at 0.094 Hz seems to be highly nonlinear compared with other CWs especially the one at 0.065 Hz. The large bispectral amplitude at (0.29, 0.066) seems to be the third harmonic contribution from the CW or CWs at 0.094 Hz whose second harmonic contributions are clubbed with the peak at (0.15, 0.066) exactly at 0.188 Hz. Even though the second order interaction peak at (0.172, 0.15) is of insignificant level compared to first order interaction peaks, it seems to be of high importance in this particular sea state since the interaction pair shows high bicoherence (>0.3) at (0.175, 0.155) in Fig. 4. This is due to a second order interaction involving the second harmonic of the highly nonlinear CW or CWs at 0.094 Hz with another small nonlinear CW at 0.159 Hz. A close look at the bispectrum and the autospectrum shows that the CWs from 0.065 (peak) to about 0.14 Hz are nonlinear in a sequence, perhaps, continuously.

The largest bicoherence peak (Fig. 4) at (0.28, 0.06) is due to the third harmonic of the highly nonlinear CW or CWs centered at 0.094 whose high nonlinearity gives rise to the second order peak at (0.175, 0.155) also. Partitioning the CW

Table 1 - Nonlinear interaction features derived from different wave profiles
(Approximate noise level is specified as the value of 25th bispectral peak)

Bispectral peaks			Bicoherence peaks			Autospectral peaks				Appr. noise	
A	B	C	A	B	C	Harmo. related	C	Others	C	Bisp.	Bicoh.
<i>Wave profile B 01</i>											
0.092	0.066	2.9	0.280	0.060	0.43	0.065	3.7	0.078	0.80		
0.290	0.066	>1.0	0.210	0.060	>0.4	0.140	0.3	0.094	0.25		
0.150	0.066	>0.7	0.220	0.060	>0.4	0.206	<0.1	0.159	0.20	0.8	0.21
0.220	0.066	>0.5	0.250	0.074	>0.3			0.228	<0.1		
0.250	0.066	>0.5	0.175	0.155	>0.3			0.275	~0.1		
			0.140	0.085	>0.3						
<i>Wave profile B 17</i>											
0.110	0.063	9.2	0.156	0.054	0.49	0.072	2.25	0.116	0.90		
0.156	0.064	>7.5	0.118	0.101	>0.4	0.134	1.80	0.172	0.80		
0.174	0.066	>6.0	0.226	0.066	>0.3	0.150	1.40	0.259	1.60		
0.067	0.048	>6.0	0.154	0.094	>0.3	0.222	0.50	0.325	0.80	5.0	0.25
0.079	0.062	>6.0	0.167	0.113	>0.3	0.243	0.90				
0.231	0.063	>6.0	0.115	0.071	>0.3	0.294	0.80				
0.167	0.113	>4.5	0.190	0.078	>0.3	0.309	1.05				
			0.254	0.054	>0.3						
<i>Wave profile B 10</i>											
0.092	0.069	3.6	0.167	0.071	0.45	0.069	1.6	0.084	0.7		
0.167	0.076	>3.5	0.153	0.137	>0.4	0.130	0.4	0.111	0.6		
0.111	0.076	>2.5	0.214	0.106	>0.4	0.150	0.9	0.247	0.2	1.8	0.2
0.111	0.094	>2.5	0.269	0.060	>0.3	0.197	0.3	0.303	0.6		
0.156	0.139	>2.0				0.281	0.4	0.325	1.3		
<i>Wave profile B 07</i>											
0.278	0.071	>6.0	0.139	0.121	>0.4	0.094	2.4	0.066	0.6		
0.247	0.103	>4.2	0.206	0.098	>0.3	0.269	3.5	0.253	1.8		
0.203	0.098	>3.3	0.247	0.098	>0.3			0.284	1.7		
0.144	0.131	>3.3	0.181	0.155	>0.3			0.309	2.0		
			0.139	0.085	>0.3					2.5	0.17
			0.139	0.060	>0.3						
			0.239	0.061	>0.3						
			0.219	0.061	>0.3						
			0.094	0.077	0.3						

A = X-axis, B = Y-axis, C = Intensity

power (0.1 m² sec) at 0.275 Hz into linear and nonlinear using the bicoherence value 0.43, it is seen that the third harmonic power is 0.04 m² sec and the linear power is 0.06 m² sec. Hence, the third harmonic is about 0.16th (0.04/0.25) of the primary CW power at 0.094 Hz. The bicoherence peak centered at (0.25, 0.074) corresponds to the fourth harmonic of the primary at 0.065 Hz. The twin peak centered at (0.20, 0.06) has a wide cross section from 0.195 to 0.23 Hz, and would cover the effects of the third harmonics of the CWs at 0.065 and 0.078 Hz. The absence of any significant bicoherence peak centered at (0.092,

0.066) corresponding to the similarly placed large and wide peak in the bispectrum (Fig. 3) is a normal occurrence in bicoherence estimates of nonlinear Stokes type profiles. In such situations the primary of the nonlinear wave would not show any bicoherence activity, even though, the bispectral maximum would be at the frequency of the primary. Otherwise, in a bicoherence spectrum the primary of a nonlinear Stokes wave would be represented as totally linear. Results from wave profile B01 alone substantiated the true nature of CWs in a sea state as nonlinear of varying degrees, many approaching to linear types.

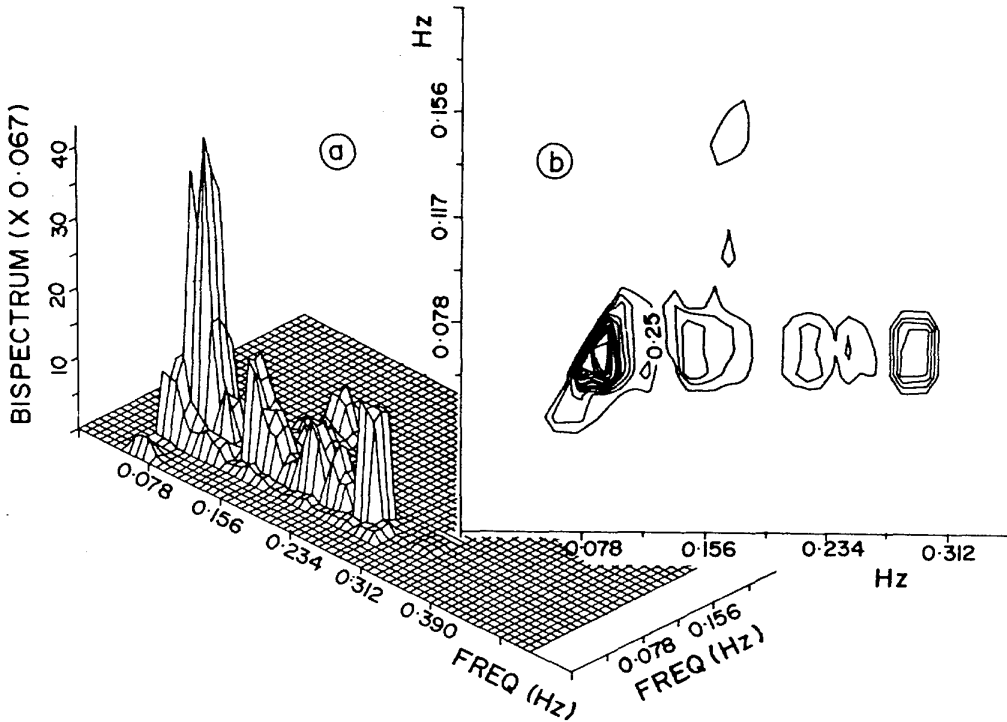


Fig. 3 - Bispectrum of B01 in two formats. [Contour interval = 0.25]

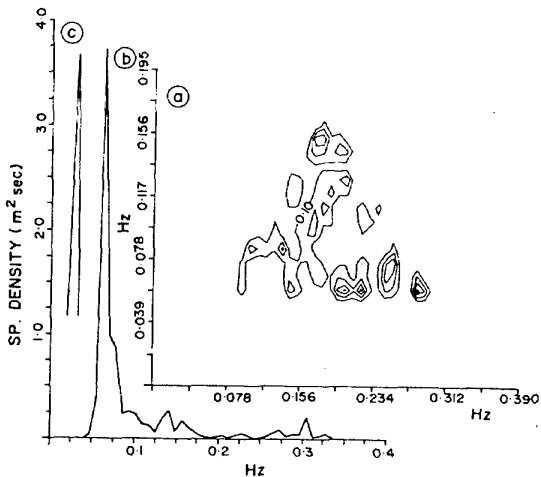


Fig. 4 - Bicoherence spectrum (a) and autospectrum (b) of B01. (c) is the structure of spectral peak of sine curve obtained through the present computing algorithm. [Contour interval = 0.1]

Profile B17—The gross features of nonlinear interaction properties (Figs 6b and 8a) of this profile are almost the same as that of B01 with some differences due to two other prominent au-

tospectral peaks centered at 0.14 and 0.26 Hz which seem to be of different origins. The bispectral cross sections (Fig. 8a) are wide enough to include many combinations of CWs in interaction. Here, the bispectral maximum is at (0.110, 0.063) corresponding to an interaction of the swell peak with a highly nonlinear CW at 0.116 Hz. The first order and second order bicoherence peaks (Fig. 6b) at (0.115, 0.071) and (0.118, 0.101) due to contributions from the CW at 0.116 Hz and second harmonic of low frequency CW in the swell regime prove that the CW at 0.116 Hz is highly nonlinear. The twin bispectral peaks at (0.156, 0.064) and (0.174, 0.066) are due to the second super harmonic of the swell peak, second subharmonic of the sea peak centered at 0.309 Hz and nonlinear CWs at 0.172 Hz. The twin peaks at (0.067, 0.048) and (0.079, 0.062) are due to peak to peak interactions of the swell CWs whose primaries do not show any bicoherence effects in Fig. 6b as expected. The bispectral peak at (0.231, 0.063) is due to contributions from the third harmonic of the swell peak and nonlinear CWs at 0.222 and 0.243 Hz. The second order peak at (0.167, 0.113) (Fig. 8a) is due to contributions from second harmonic of the swell peak and

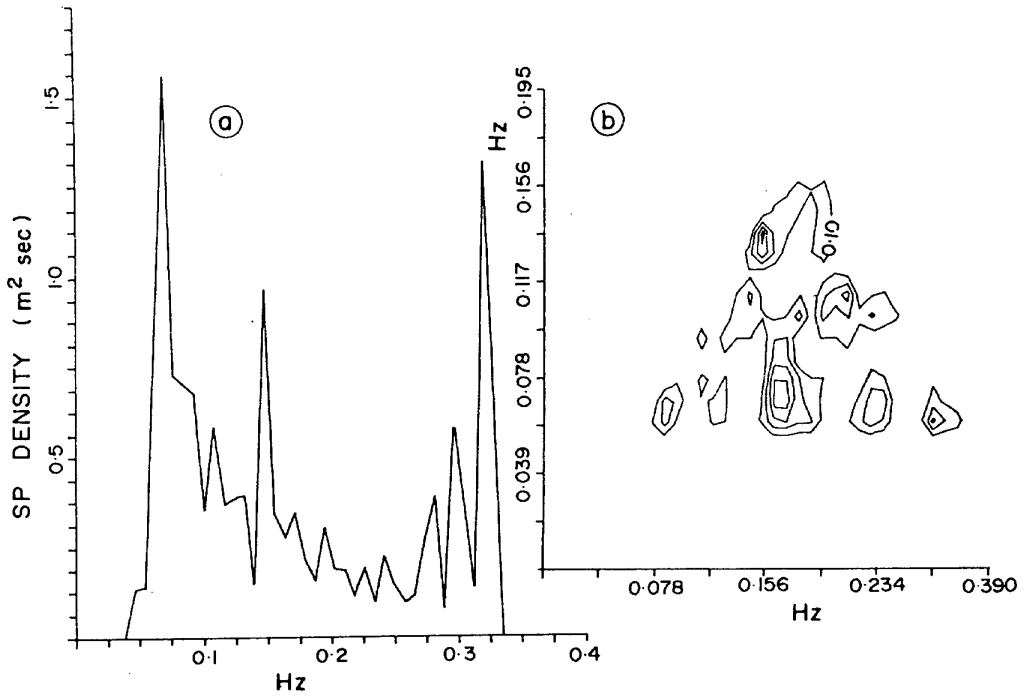


Fig. 5 – Bicoherence spectrum (b) and autospectrum (a) of B 10. [Contour interval = 0.1]

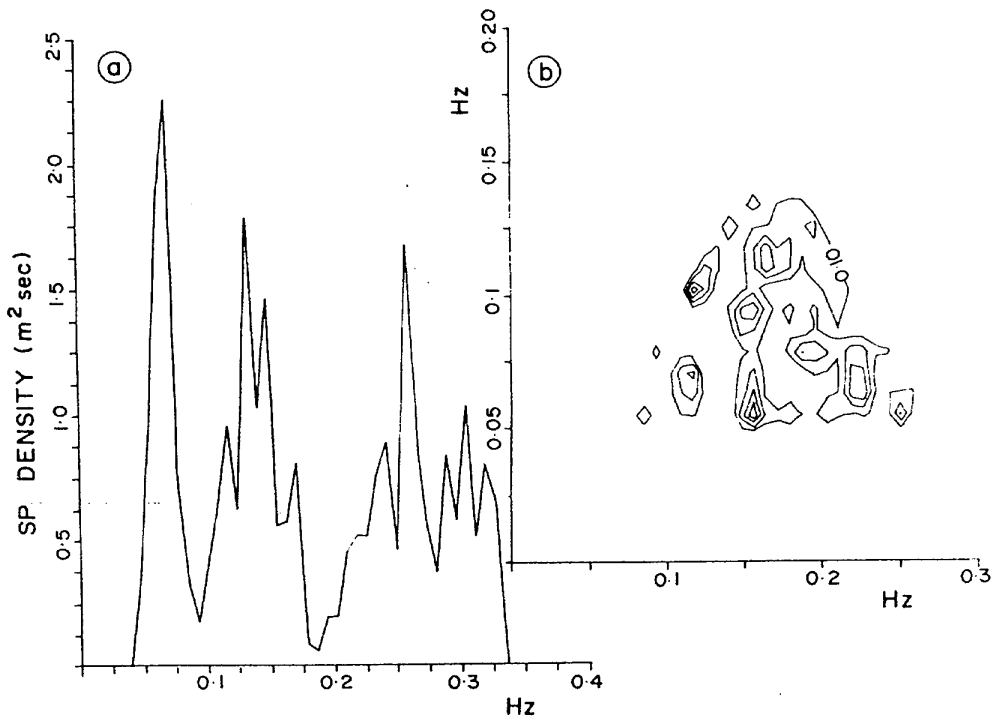


Fig. 6 – Bicoherence spectrum (b) and autospectrum (a) of B 17. [Contour interval = 0.1]

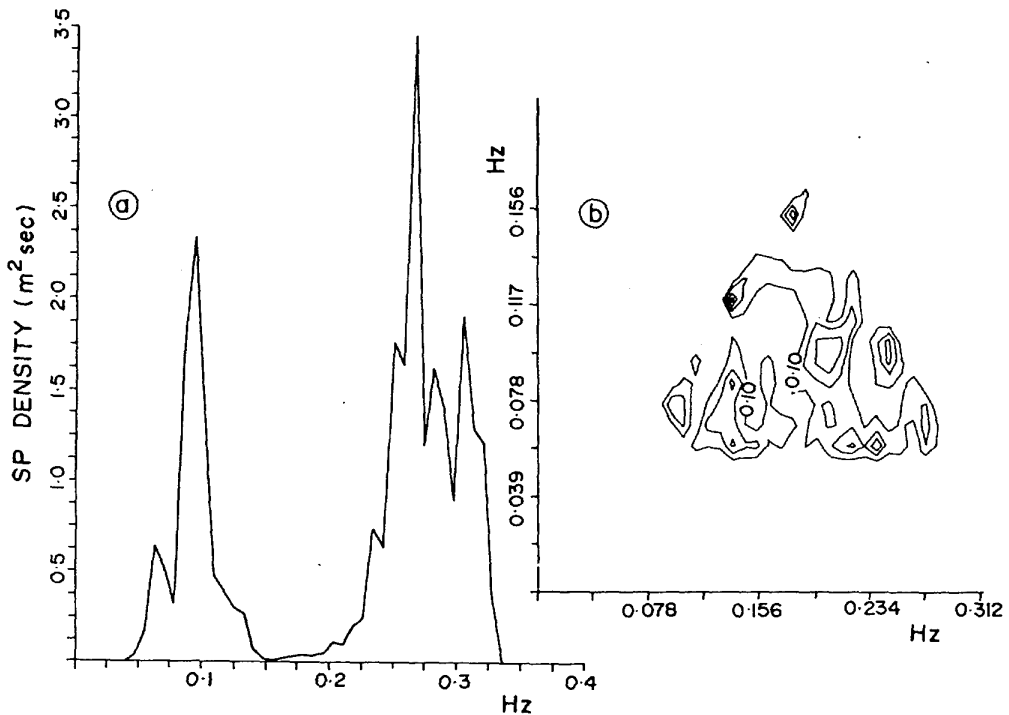


Fig. 7 - Bicoherence spectrum (b) and autospectrum (a) of B 07. [Contour interval = 0.1]

the highly nonlinear CW at 0.116 Hz. The bicoherence peaks (Fig. 6b) at (0.156, 0.054), (0.226, 0.066), (0.115, 0.071), (0.254, 0.054) and (0.190, 0.078) are all due to higher order (2nd, 3rd and 4th harmonics) contributions of the swell peak combined with the subharmonic contributions from the nonlinear CWs at higher frequencies. The peaks at (0.118, 0.101), (0.154, 0.094) and (0.167, 0.113) are due to second order interactions involving higher harmonics of nonlinear CWs. It is worth noting here that B17 was recorded about 50 h after B01 during which interval the swell peak largely weakened twice and later grew to B17 stage.

Profile B10 - The main bispectral peak (Fig. 8b) at (0.092, 0.069) with its subpeaks at (0.111, 0.076) and (0.111, 0.094) includes a peak to peak interaction of the swell regime with its high frequency side band CWs upto 0.111 Hz. This peak is similar to those observed for B01 and B17. This group of swell CWs are seen to be very nonlinear from the bispectral peak centered at (0.167, 0.076) which corresponds to the second harmonic of the CWs of the swell peak. The peak at (0.156, 0.139) is due to second order interaction of the highly nonlinear CW at 0.15 Hz whose first order interaction peak is merged at (0.167, 0.076) with

the second harmonic of the swell CWs. The largely nonlinear nature of the CWs of the swell regime is demonstrated again by the absence of a significant bicoherence value (Fig. 5b) for frequency range < 0.13 Hz. The two bicoherence peaks at (0.153, 0.137) and (0.167, 0.071) demonstrates the highly nonlinear nature of the CW at 0.15 Hz and the large second harmonic contributions of the swell CWs, respectively. The peak at (0.214, 0.106) in Fig. 5b shows a second order contribution from the swell CWs. The peak at (0.269, 0.06) seems to be the combined effects of higher harmonics of CWs in the swell regime and at 0.15 Hz. Absence of bicoherence contributions over many intervals on frequency axis shows that over these intervals the CWs approach to linear waves.

Profile B07 - This bispectrum (Fig. 8c) is characteristically different showing its maximum peak at (0.278, 0.071) in the dominant sea regime whereas all the previous bispectra show their peaks in the swell domain. This peak is due to the highly nonlinear CWs in the sea regime. The peak at (0.144, 0.131) is a second order interaction peak involving the second subharmonics of the highly nonlinear CWs in the sea domain. The peaks at (0.247, 0.103) and (0.203, 0.098) are due to interactions involving the second and third

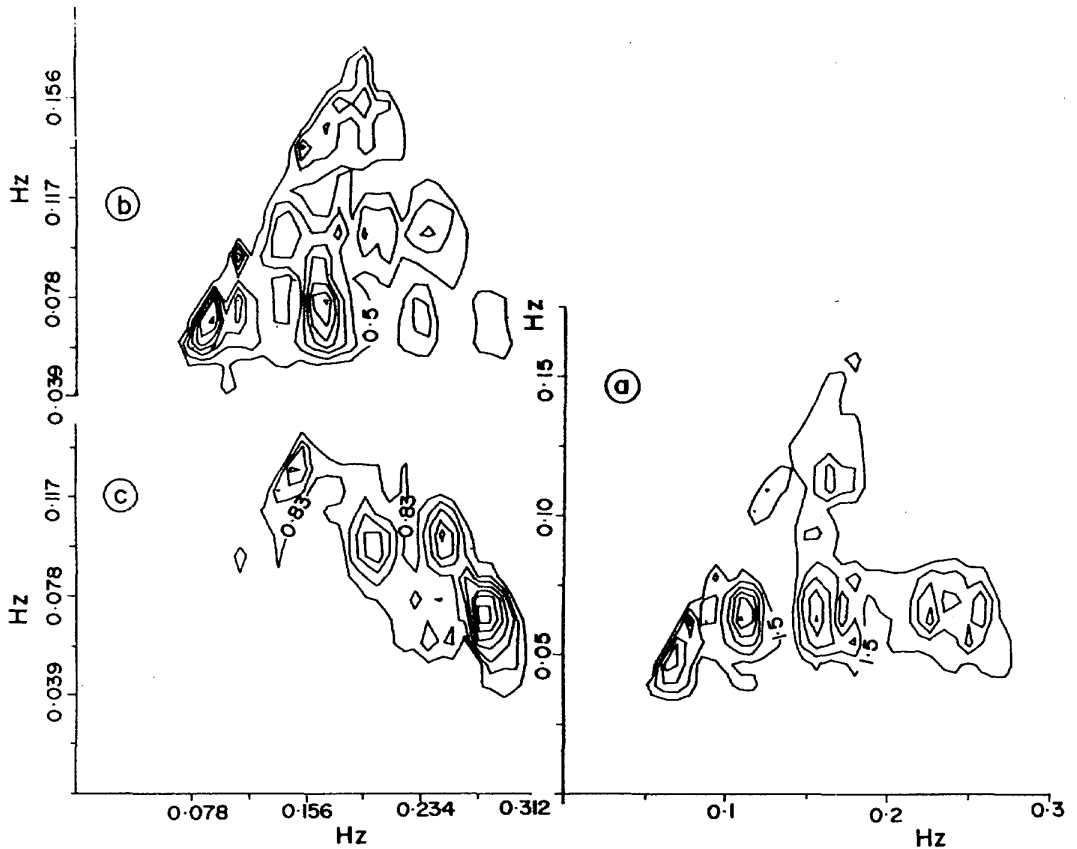


Fig. 8 - Bispectra of B 17 (a) B 10 (b) and B 07 (c). [Contour intervals are same as outer contour values]

harmonics of the nonlinear CWs in the swell domain. The absence of peak to peak interaction (Fig. 8c) for the swell CWs indicates that its intensity is of no significance compared to the bispectral intensity in the sea regime. The oblong shaped contours in the sea regime seems to be an effect of the wide sea domain with considerable energy from 0.25 to 0.32 Hz.

The most important feature to be noted in the bicoherence spectrum of B07 (Fig. 7b) is the presence of a peak at (0.094, 0.077). The bicoherence spectra of swell dominated sea states (Figs 4, 5 and 6) do not show a peak for the swell regime similar to Stokes nonlinear profiles in which the primary does not show bicoherence peak. Contrary to that, the presence of a bicoherence peak at (0.094, 0.077) for B07 shows that the CWs in the sea regime have significant subharmonic contributions. Interpreting the CWs in the sea regime in a different way (but similar to swell CWs with large period, low amplitude primaries and low period large amplitude super harmonics),

the sea CWs are visualised to be very much nonlinear compared to the CWs in the swell regime, making the sea state very steep and breaking (see wave statistics presented in Table 2). The second order bicoherence peak at (0.139, 0.121) is due to contributions from second subharmonics of CWs in the sea regime. Another second order peak at (0.181, 0.155) arises from the second super harmonics of the CWs of the swell regime. Some mixed effects of subharmonics and super harmonics also can be expected in the peaks. The peaks at (0.206, 0.098) and (0.247, 0.098) are also second order peaks involving the swell CWs and their second and/or third super harmonics. Peaks at (0.139, 0.085), (0.139, 0.060), (0.239, 0.061) and (0.219, 0.061) represent nonlinear contributions arising out of first order interactions involving super harmonics of swell CWs and CWs in the sea regime.

The most striking feature in the bicoherence spectra is the presence of nonlinear CW power all over the frequency axis arising from first and sec-

ond order interactions. The effect of second order contributions increases as the spectra changes from swell dominated (B01) to sea dominated (B07). This indicates that multisourced and sea dominated sea states would generally be highly nonlinear compared to single sourced swell systems, possibly due to breaking. The above description involving 4 very widely varying sea states clearly substantiates the proposed hypothesis of nonlinear CWs as the real physical constituents of deep water sea states.

From the volumes of real and imaginary parts (Table 2) of the bispectra of the different profiles it is very clear that a correct and full representation of nonlinear interaction properties is possible only by the modulus of bispectrum. Masuda & Kuo^{33,34} showed that the values of imaginary parts of bispectrum are very different for sea states in decaying and generating areas; 20% and 50% of real part respectively. From the results presented above it seems that the nonlinearity of a sea state can be resolved into two parts; one arising out of steepening of wave crests (Stokes type) resulting in horizontal asymmetries between crest and trough and the second arising out of deformation of wave crests and troughs resulting in vertical asymmetries within crests and troughs. The first one is mainly caused by coupled nonlinear generation by mean wind and the second by tangential stress and sheltering effects. These two processes do not seem to be completely independent. The statistics presented in Table 2 seem to support the idea. In the swell dominated sea states the percentage volumes of imaginary parts varied from 49 to 138. Sea state B10 has a value of 138% whose autospectrum has two or more Stokes type CWs centered at 0.069 and 0.15 Hz. B01 has a value of 125% with only one peak of Stokes type CW. B17 is multisourced but dominated by swell, but the effect of high frequency waves associated with second type of nonlinearity seems to dominate the scene. Lastly, B07 has -82% imaginary part volume with positive real part which seems to in-

dicate that nonlinearity induced by sheltering and tangential stress on high, steep nonlinear waves are comparatively high resulting in breaking and making the first type of nonlinearity insignificant (also seen from the bispectrum in Fig. 8c). A casual study of statistics for B07 in Table 2 demonstrates other supporting characteristics for a steep, breaking sea state.

Generation, growth and nonlinearity in relation to the hypothesis—It is evident from the above discussion and Table 2 that volumes of real and imaginary parts have something very remarkable to do with different types of sea states like swells, seas at various stages of development and swell and sea mixed with different intensities. Hence, it is clear that different energy transfer mechanisms from wind during different phases of generation and growth would also play different roles in deciding the bispectral structure. Various wave generation theories available in literature do not model the various physical processes individually and completely. Each one stresses some phase of evolution of sea state. Hence, combined models are developed to describe the whole physical processes. Miles by combining Phillip's resonance model and his own shear flow model described³⁵ the whole evolution scene with an initial linear phase, an exponential growing phase and a final linear phase leading to fully developed and intensely breaking situations. The effects of sheltering and tangential stress are not included in the combined model but now seems to be important in the light of the discussion on the relative significance of real and imaginary parts of different sea states. Now, it seems to be possible to delineate the different phases of sea state evolution as follows with some vague tags of different nonlinear processes to different phases of growth.

(1) In the stage of initial generation of wavelets and their groups involving Phillip's resonance mechanism and skin flow, effect of sheltering and tangential stress is insignificant as the wind is weak and unsteady and waves are low. This initial

Table 2 - Some important statistics of the different wave profiles with volumes of real and imaginary parts. [CS = Hr.m.s/(1.5*T₀₂), where T₀₂ is mean zero-crossing period from 0th and 2nd spectral moments]

Wave profile	Highest wave (m)	Highest wave's period (sec)	Ch. Steep. (CS)	No. of all crests (NC)	No. of zero-cross. waves (Nz)	Mean crest per. (sec)	Mean zero-cross per. (sec)	Mean height (m)	Sig. height (m)	Bispectral vol.	
										Real	Imag.
B 01	1.10	14.6	0.01	71	60	10.9	12.9	0.59	0.91	-0.0109	-0.0136
B 17	1.92	4.7	0.03	136	93	6.3	9.2	0.98	1.35	-0.0719	-0.0351
B 10	1.68	3.2	0.02	113	90	7.5	9.4	0.75	1.08	-0.0135	-0.0186
B 07	2.01	3.6	0.05	148	91	5.2	8.5	0.85	1.26	+0.0594	-0.0489

sea state is only very weakly nonlinear due to nascent nonlinear nature of the basic wavelets and their groups. This represents the first linear phase of evolution.

(2) The wind grows and stabilises further. Coupled wave generation by mean flow starts and steadily grows with the wind. Simultaneously tangential stress and sheltering also becomes important. Coupled generation seems to impart Stokes type nonlinearity contributing to the imaginary part. But sheltering and tangential stress deform the surface waves horizontally and seem to add to the real part. The wave period and amplitude increases due to coupled energy transfer. Nonlinear transfer by wave-wave interaction occurs significantly. This stage represents the lower half of the exponential phase of evolution. White capping and turbulence comes into play.

(3) Next stage of growth of sea is highly nonlinear by coupled energy transfer by mean wind which has grown further. Nonlinear transfer by wave-wave interaction becomes more important. Dissipation is by intense breaking. This stage represents the second half of the exponential phase of growth. Sheltering and tangential stress becomes more intense compared to the previous stage. The real and imaginary parts might show large changes within very short times due to intense breaking.

(4) This stage is the final linear phase of evolution leading to fully developed sea states with a dynamic equilibrium of all physical processes. But the energy transfer mechanisms which were significant at the first stage becomes relatively unimportant.

Acknowledgement

Author thanks Dr. J.S. Sastry, for encouragement.

References

- Anonymous, *Shore protection manual*, Vol. 1, (US Government Printing Office, Washington DC) 1975, 2.
- Osborne A R, Petti M, Liberatore G & Cavaleri L, in *Computer modelling in ocean engineering*, edited by B A Schrefler & O C Zienkiewicz, (Balkema, Rotterdam) 1988, 99.
- Kawai S, *Fluid Mech*, 93 (1979) 661.
- Hatori M, *Oceanogr Soc Japan*, 40 (1984) 1.
- Hatori M, *J Oceanog Soc Japan*, 40 (1984) 12.
- Tokuda M & Toba Y, *J Oceanog Soc Japan*, 37 (1981) 13.
- Toba Y, in *Naval hydrodynamics*, Proc. 12th Symp. (National Academy of Sciences, Washington DC) 1979, 529.
- Phillips O M, in *Turbulent fluxes through the sea surface, wave dynamics and prediction*, edited by A Favre & K Hasselmann, (Plenum Press, New York) 1978, 373.
- Phillips O M, *Proc Symp on measuring ocean waves from space* (Johns Hopkins University, Baltimore) 1987, 7.
- Lake B M & Yuen H C, *J Fluid Mech*, 88 (1978) 33.
- Rikiishi K, *J Phys Oceanogr*, 8 (1978) 518.
- Ramamonjarisova A, Baldy S & Choi I, in *Turbulent fluxes through the sea surface, wave dynamics and prediction*, edited by A Favre & K Hasselmann, (Plenum Press, New York) 1978, 403.
- Mitsuyasu H, Kuo Yi-Yu & Masuda A, in *Turbulent fluxes through the sea surface, wave dynamics and prediction*, edited by A Favre & K Hasselmann, (Plenum Press, New York) 1978, 221.
- Kitaigorodskii S A, *Proc symp on measuring ocean waves from space*, (Johns Hopkins University, Baltimore) 1987, 11.
- Hasselmann K, Barnett T P, Bouws E, Carlson H, Cartwright D E, Enke K, Ewing J A, Gienapp H, Hasselmann D E, Kruseman P, Meerburg A, Muller P, Olbers D J, Richter K, Sell W & Walden H, *Measurement of wind wave growth and swell decay during the Joint North Sea Wave Project (JONSWAP)*, Reihe A (8^o), Nr. 12, (Deutsches Hydrographisches Institut, Hamburg) 1973, pp. 95.
- Masuda A, Kuo Yi-Yu & Mitsuyasu H, *J Fluid Mech*, 92 (1979) 717.
- Tokuda M & Toba Y, *J Oceanog Soc Japan*, 38 (1982) 8.
- Yefimov V V, Soloviyev Yu P & Khristoforov G N, *Izvest Atmos Ocean Phy*, 8 (1972) 246.
- Huang N E & Chi-chao Tung, *J Fluid Mech*, 75 (1976) 337.
- Mitsuyasu H, Kuo Yi-Yu & Masuda A, *J Fluid Mech*, 92 (1979) 731.
- Lake B M, Yuen H C, Rungaldier H & Ferguson W E, *J Fluid Mech*, 83 (1977) 49.
- Lake B M & Yuen H C, *J Fluid Mech*, 83 (1977) 75.
- Elgar S & Guza R T, *J Fluid Mech*, 167 (1986) 1.
- Varkey M J, *Indian J Mar Sci*, 18 (1989) 177.
- Varkey M J, *Indian J Mar Sci*, 17 (1988) 189.
- Varkey M J, *Indian J Mar Sci*, 20 (1991) 93.
- Hasselmann K, Munk W & MacDonald G, in *Scripps Institute of Oceanography, Coll. Reprints*, Vol. 33, Contribution No. 1477 (1963) 73.
- Houmb O G, *Proc 10th Coastal Engineering Conference*, Vol. 1, (American Society of Civil Engineers, New York) 1974, 301.
- Kim Y C & Powers E J, *IEEE Transactions on Plasma Sci*, PS-7 (1979) 120.
- Elgar S & Guza R T, *J Fluid Mech*, 161 (1985) 425.
- Borgman L E, 1976, *The statistical anatomy of ocean wave spectra*, Tech. Paper No. 76-10 (Coastal Engineering Research Centre, U.S. Army Corps of Engineers) 1976, pp. 102.
- Bendat J S & Piersol A G, 1971, *Random data: analysis and measurement procedures*, (Wiley Interscience, New York) 1971, pp. 407.
- Masuda A & Kuo Yi-Yu, *Deep-Sea Res*, 28A (1981) 213.
- Masuda A & Kuo Yi-Yu, *Deep-Sea Res*, 28A (1981) 223.
- Kinsman B, *Wind waves: their generation and propagation on the ocean surface*, (Prentice-Hall Inc., New Jersey) 1965, pp. 676.